Revascularization of swine renal artery stenosis improves renal function but not the changes in vascular structure

Frederic Favreau[1,2], Xiang-Yang Zhu[1], James D. Krier[1], Jing Lin[1], Lizette Warner[1], Stephen C. Textor[1] and Lilach O. Lerman[1]

[1]*Division of Nephrology and Hypertension, Department of Medicine, Mayo Clinic, Rochester, Minnesota, USA*

Renal revascularization by percutaneous transluminal angioplasty improves blood pressure and stenotic kidney function in selected groups of patients, but the reversibility of intrarenal and microvascular remodeling remains unknown. Here, we tested the hypothesis that renal angioplasty improves the function and structure of renal microcirculation in experimental chronic renal artery stenosis. Stenotic kidney function, hemodynamics, and endothelial function were assessed *in vivo* in pigs after 10 weeks of unilateral renal artery stenosis. Renal microvascular remodeling, angiogenic pathways, and fibrosis were measured *ex vivo*. Angioplasty and stenting carried out 4 weeks before measurement decreased blood pressure, improved glomerular filtration rate, and improved microvascular endothelial function. It also promoted the expression of angiogenic factors and decreased renal apoptosis due to stenosis, compared with a sham intervention. The spatial density of renal microvessels, however, was partially improved after angioplasty. Renal blood flow was incompletely restored compared with the kidneys of sham-treated animals, as was interstitial fibrosis. Renal microvascular media-to-lumen ratio remained unchanged by angioplasty. Thus, our study shows that revascularization of a stenotic renal artery restores the glomerular filtration rate and renal endothelial function 4 weeks later. Renal hemodynamics and structure, however, are incompletely resolved.

Kidney International (2010) **78,** 1110–1118; doi:10.1038/ki.2010.142; published online 12 May 2010

KEYWORDS: renal artery stenosis; renal hypertension; renovascular disease; revascularization

Correspondence: *Lilach O. Lerman, Division of Nephrology and Hypertension, Mayo Clinic, 200 First Street SW, Rochester, Minnesota 55905, USA. E-mail: lerman.lilach@mayo.edu*

[2]Current address: Inserm U927, Poitiers F-86000, France; or Faculte de Medecine et de Pharmacie, Université de Poitiers, Poitiers F-86000, France; or Service de Biochimie, CHU Poitiers, Poitiers F-86000, France.

Received 6 October 2009; revised 22 February 2010; accepted 16 March 2010; published online 12 May 2010

Renal artery stenosis (RAS) induced mainly by atheromatous disease can accelerate hypertension and renal failure[1] and lead to adverse cardiovascular outcomes. The main treatment options for RAS include medical therapy and/or revascularization of the stenotic renal artery aimed to improve blood pressure control and preserve renal function.

The role of percutaneous transluminal renal angioplasty (PTRA), followed by stenting of the revascularized renal artery and optimal medical therapy, remains controversial. Although restoration of kidney perfusion should restore renal function and improve blood pressure control, several prospective, randomized trials up to now fail to identify compelling benefits for cardiovascular or kidney outcomes.[2] Notably, most studies in humans evaluating the response to PTRA are limited to changes in serum creatinine, glomerular filtration rate (GFR), blood pressure, or number of medications.[3,4]

Obstruction of flow in the renal artery initiates a complex cascade of events that remains incompletely understood. Using a swine model of progressive RAS, we have previously shown that the kidney exposed to chronic RAS shows functional deterioration accompanied by renal inflammation, fibrosis, and microvascular rarefaction and remodeling.[5–8] Diminished intrarenal microvascular density may be the result of either altered or insufficient angiogenesis with or without acceleration of apoptosis. It is associated with impaired renal function and structure.[8] However, little is known about the ability of revascularization to restore the renal microcirculation and attenuate microvascular injury.

The aims of this study were to explore the effect of PTRA and stenting on intrarenal microvascular remodeling, angiogenesis, and fibrosis. To test the hypothesis that PTRA can modify the function and structure of renal microcirculation in the stenotic kidney, we used a large animal model of chronic experimental RAS. The pigs underwent revascularization with PTRA and stenting after 6 weeks of unilateral RAS, a duration associated with the development of renovascular hypertension, kidney dysfunction, and renal fibrosis.[9–11] They were studied *in vivo* 4 weeks later, to allow for detectable improvement of renal and endothelial functions.[12,13]

RESULTS

Systemic and hemodynamic parameters

At 6 weeks after coil implantation, hemodynamically significant RAS (>60%) was present in all pigs (Figure 1a and b). PTRA was successfully performed in six pigs (degree of stenosis before PTRA 68.3 ± 4.4%) and was followed by a decrease of mean arterial pressure (MAP) to the baseline level (Figure 1c), whereas the remaining RAS pigs (degree of stenosis 71.5 ± 6.3%, P = NS) had sham angiography. Sham-treated RAS group still had significant stenosis (75.3 ± 5.9%) and elevated systolic blood pressure ($P<0.05$ vs sham) 4 weeks later, and MAP tended to increase as well ($P=0.068$), whereas in RAS + PTRA group the renal artery was patent with a minimal residual stenosis (Table 1). Blood pressure after PTRA was lower than untreated RAS group and not different from sham-treated group (Table 1). Creatinine levels slightly increased in RAS group and were lower after PTRA, whereas plasma renin activity was not different among the groups (Table 1).

Renal hemodynamics and function

At 10 weeks after induction of RAS, basal GFR and renal blood flow (RBF) were significantly lower in the RAS kidney compared with sham and the response to acetylcholine (Ach) was attenuated (Figure 1d), indicating endothelial dysfunction. In the RAS + PTRA group, GFR was improved and not different from sham, whereas RBF was not significantly higher than RAS and remained lower compared with sham ($P<0.05$). Nevertheless, both GFR and RBF responses to Ach were improved ($P=0.016$ and $P=0.001$ vs baseline, respectively), suggesting an improvement of endothelial function after PTRA. The slight decrease in renal volume in RAS was partially reversed by PTRA, but this did not reach statistical significance because of a high variability (Table 1). Cortical perfusion, which tended to decrease in RAS, reached statistical significance in RAS + PTRA group ($P<0.01$ vs sham, Table 1) and was not different between the two RAS groups.

Microvascular three-dimensional architecture and remodeling

Overall, transmural spatial density of renal microvessels across the cortical regions was lower in RAS ($P<0.01$ vs sham) and improved in RAS + PTRA (Table 2, Figure 2a and b, $P>0.05$ vs sham), whereas average vessel diameter was unchanged ($P=0.7$). Microvascular tortuousity tended to increase in both RAS and RAS + PTRA ($P=0.12$), suggesting angiogenic activity to restore microvessels (Table 2). In addition, small microvessels with a diameter under 40 µm were reduced in RAS ($P<0.001$ vs sham) and improved by

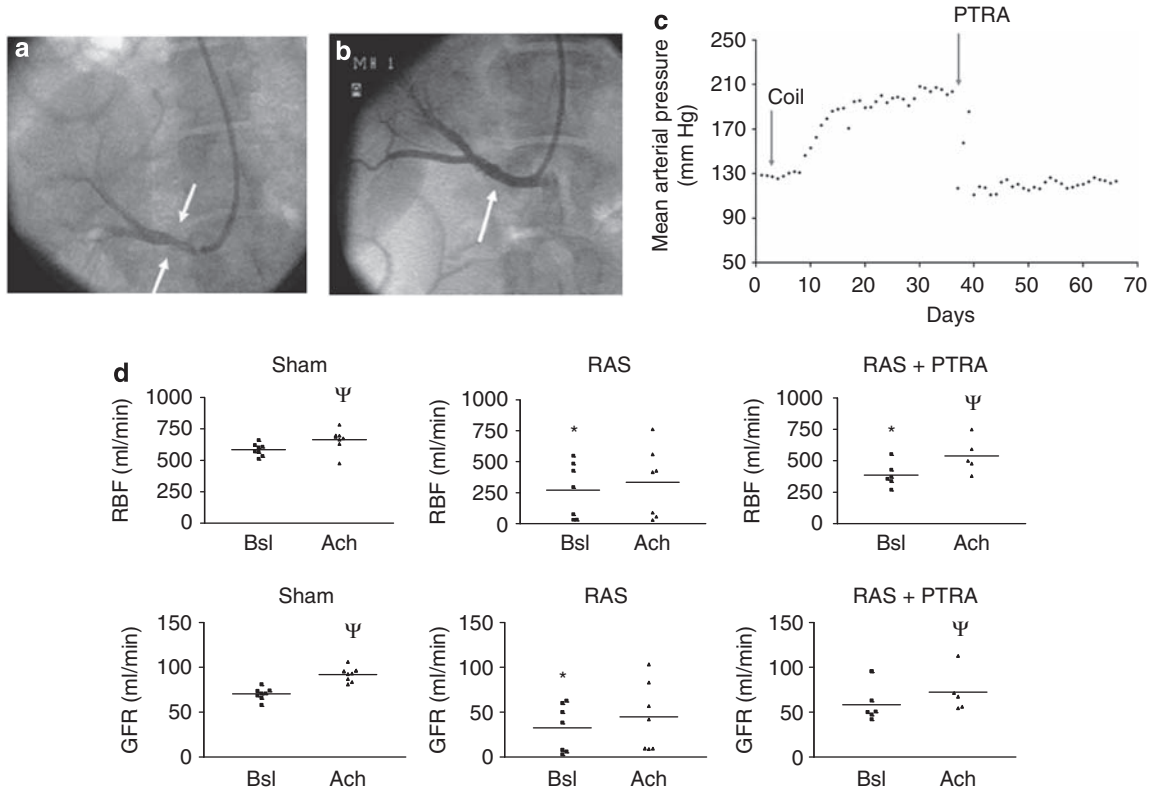

Figure 1 | Effect of PTRA on blood pressure and renal function. Renal angiography in a pig with renal artery stenosis (RAS) before (**a**) and 4 weeks after (**b**) revascularization with percutaneous transluminal renal angioplasty (PTRA) and stenting. Arrows indicate the location of the stenosis before and after PTRA. (**c**) Representative evolution of mean arterial pressure measured using telemetry in a RAS pig after implantation of a local-irritant coil. RAS increased blood pressure, which rapidly returned to baseline levels after PTRA. (**d**) Single-kidney renal blood flow (RBF) and glomerular filtration rate (GFR) at baseline (Bsl) and in response to acetylcholine (Ach). *$P<0.05$ vs sham, $^{\Psi}P<0.05$ vs Bsl.

Table 1 | Systemic characteristics and basal single-kidney hemodynamics (mean ± s.e.m.) in sham, sham-treated renal artery stenosis (RAS), and RAS pigs 4 weeks after PTRA

	Sham	RAS	RAS+PTRA
Number of kidneys	8	7	6
Body weight (kg)	47.5 ± 1.5	56.0 ± 3.0	54.5 ± 3.4
Diastolic blood pressure (mm Hg)	88.3 ± 4.0	107.6 ± 8.3	94.5 ± 8.1
Systolic blood pressure (mm Hg)	111.5 ± 3.5	139.3 ± 9.6*	122.3 ± 10.3
Mean arterial pressure (mm Hg)	96.0 ± 3.8	118.1 ± 8.6	103.8 ± 8.9
Degree of stenosis (%)	0	75.3 ± 5.9*	5.0 ± 3.4§
PRA (ng/ml/h)	0.25 ± 0.04	0.22 ± 0.05	0.25 ± 0.14
Creatinine (mg/dl)	1.15 ± 0.09	1.5 ± 0.08*	1.28 ± 0.12
Basal RBF (ml/min)	584.8 ± 17.118	271.0 ± 84.5*	386.1 ± 39.5*
Basal GFR (ml/min)	70.4 ± 2.4	32.7 ± 10.0*	58.2 ± 8.0
Ach-RBF (ml/min)	663.8 ± 30.9$^{\Psi}$	334.0 ± 106.9*	539.7 ± 62.4$^{\Psi}$
Ach-GFR (ml/min)	91.9 ± 2.8$^{\Psi}$	44.8 ± 14.5*	72.4 ± 10.6$^{\Psi}$
Renal volume (ml)	123.9 ± 3.7	79.9 ± 21.0	114.1 ± 11.2
Cortical perfusion (ml/min/cc tissue)	4.96 ± 0.11	3.85 ± 0.43	3.78 ± 0.23*

Abbreviations: Ach, acetylcholine; GFR, glomerular filtration rate; PRA, plasma renin activity; PTRA, percutaneous transluminal renal angioplasty; RBF, renal blood flow.
*$P<0.05$ vs sham; $^{\Psi}P<0.05$ vs basal values; $^{\S}P<0.05$ vs RAS.

Table 2 | Renal cortical microvascular architecture assessed by micro-CT in sham, sham-treated renal artery stenosis (RAS), and RAS+PTRA pigs

	Sham	RAS	RAS+PTRA
Spatial density (vessels/mm^2)	2.70 ± 0.24	1.50 ± 0.15*	1.97 ± 0.06
Average vessel diameter (μm)	91 ± 4	102 ± 12	95 ± 9
Tortuousity (ratio)	1.30 ± 0.04	1.43 ± 0.05	1.51 ± 0.12

Abbreviations: micro-CT, micro-computed tomography; PTRA, percutaneous transluminal renal angioplasty.
Values are means ± s.e.m. *$P<0.05$ vs sham.

PTRA ($P>0.05$ vs sham). The density of 40–100 μm microvessels tended to be reduced in RAS and RAS + PTRA ($P=0.073$ vs sham), whereas larger microvessels were unaffected in either group (Figure 2).

The expression of vascular endothelial growth factor (VEGF) ($P<0.05$ vs sham) and Flt-1 ($P<0.05$ vs sham) increased in RAS, and Flk-1 tended to increase as well ($P=0.1$, Figure 3). In RAS + PTRA, VEGF increased further ($P<0.01$ vs RAS), whereas Flt-1 and Flk-1 both decreased to normal levels (Figure 3). In addition, angiopoietin-1 expression was upregulated after PTRA ($P<0.01$ vs RAS, Figure 3), whereas endothelial nitric oxide synthase was unchanged. Moreover, matrix metalloproteinase-2 was increased in RAS ($P<0.05$ vs sham, Figure 3), but further elevated in RAS + PTRA ($P<0.001$ vs RAS, Figure 3), whereas the expression of its inhibitor, tissue inhibitors of metalloproteinase 2 (TIMP-2), was similarly blunted in both groups ($P<0.01$ vs sham). The expression of tissue transglutaminase in RAS and RAS + PTRA groups was not significantly different from sham ($P=0.18$, Figure 3). Increase in microvascular media-to-lumen ratio in RAS and RAS + PTRA groups compared with sham ($P<0.001$ vs sham) indicated microvascular remodeling that was not reversed 4 weeks after PTRA (Figure 4).

Renal tissue remodeling

Renal artery stenosis showed increased renal apoptosis (fraction of terminal deoxynucleotidyl transferase dUTP nick end labeling (TUNEL)-positive cells) compared with sham ($P<0.01$, Figure 5), in association with increased expression of activated caspase-3. Both indices of apoptosis were significantly attenuated after PTRA, although activated caspase-3 expression remained higher than that in sham (Figure 5).

In addition, trichrome staining (indicating renal fibrosis) increased in RAS ($P<0.01$ vs sham, Figure 6), and was unaffected by PTRA ($P<0.05$ vs sham, Figure 6). Moreover, cortical hydroxyproline content, reflecting collagen content, was elevated in the RAS group (16.4 ± 3.6 vs 5.3 ± 0.8 μg per 10 mg, $P=0.01$ vs sham), and decreased but not normalized after PTRA (8.5 ± 0.4 μg per 10 mg, $P=0.018$ vs RAS, $P=0.002$ vs sham, Figure 6). There were no detectable differences in the expressions of transforming growth factor-β and TIMP-1 among the groups ($P=0.30$ and $P=0.39$, respectively, Figure 6), but connective tissue growth factor expression tended to increase in RAS group and was statistically significantly elevated in RAS + PTRA group ($P<0.05$ vs sham, Figure 6). The expression of xanthine oxidase increased in the RAS kidney ($P<0.05$ vs sham) and decreased to sham levels after PTRA ($P<0.05$ vs RAS, Figure 6), suggesting attenuation of oxidative stress induced by RAS.

DISCUSSION

This study shows that PTRA performed after 6 weeks of experimental RAS partially restored GFR and renal endothelial function. These changes were associated with enhanced proliferation and maturation of new vessels, but renal perfusion, vascular wall remodeling, and interstitial fibrosis remained incompletely restored. Our study therefore shows that PTRA in swine RAS can only partially restore the renal microcirculation. Importantly, these observations suggest that meaningful improvement in GFR could be achieved without complete reversal of renal tissue remodeling.

Our results extend clinical observations in human subjects with atherosclerotic renal artery disease. Hemodynamically significant RAS (>60% decrease in luminal diameter) is

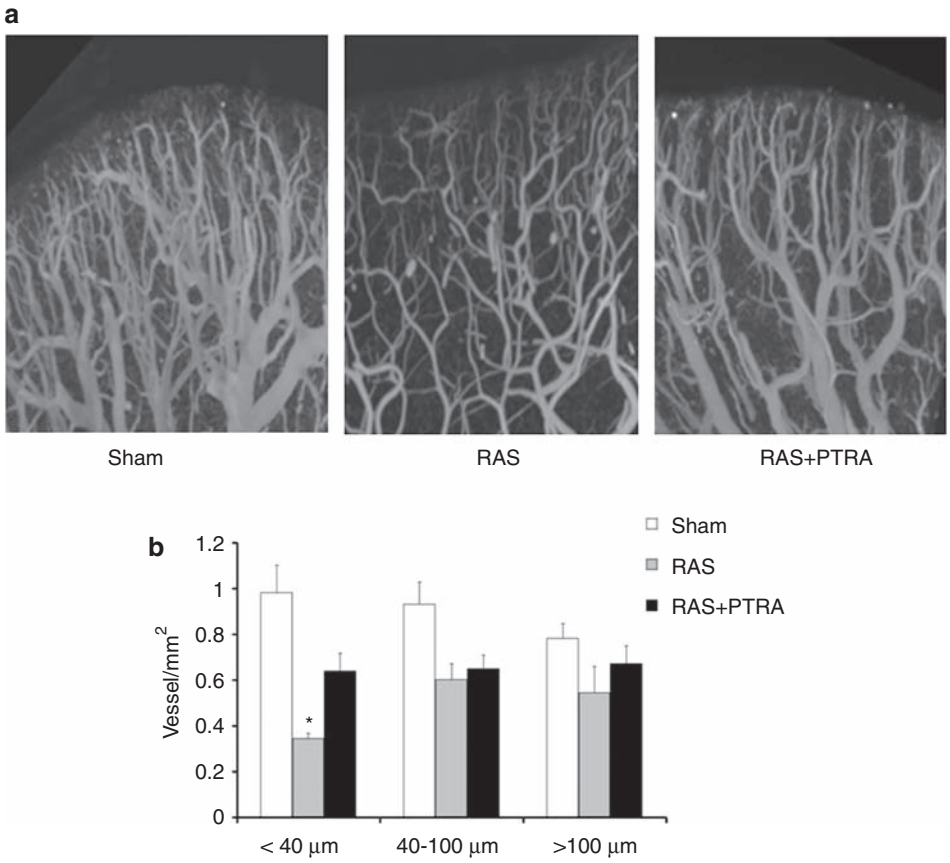

Figure 2 | The kidney microcirculation before and after revascularization of a stenotic renal artery. Representative three-dimensional tomographic images of the cortical microcirculation in sham, renal artery stenosis (RAS), and RAS + percutaneous transluminal renal angioplasty (PTRA) pigs (**a**) and spatial density (**b**, mean ± s.e.m.) of different size microvessels. PTRA slightly increased intrarenal density of small microvessels. *$P<0.05$ vs sham.

detected in almost 7% of individuals older than 65 years of age.[14] RAS regularly accelerates renovascular hypertension, renal dysfunction, and increased cardiovascular mortality. Revascularization of the kidney using PTRA or other means can lead to a decrease in blood pressure, and in turn to an improvement in the systemic endothelial function and oxidative stress.[12] Remarkably, renal function improves only in a minority of patients with atherosclerotic RAS.[1] However, the reasons for incomplete recovery of renal function in RAS remain obscure.[2]

In our experimental swine model, arterial pressure increased within a few days after implantation of a local-irritant coil as a result of a significant RAS. We have previously shown that this is associated with a decrease in GFR and RBF,[9,15] and with renal endothelial dysfunction.[10,16] Plasma renin activity is not necessarily elevated, as typical for a chronic phase of untreated renovascular hypertension,[17] implicating recruitment of alternative pressor mechanisms that maintain hypertension.[1] Our current studies with effective PTRA induced a rapid and stable decrease of arterial pressure, and by 4 weeks after PTRA, renal function (GFR and serum creatinine) improved as well. RBF improved only slightly, although not significantly, but its response to Ach was restored, suggesting improvement of endothelial function that was impaired in RAS. Notably, the reduction in pressure distal to RAS leads to decreased vascular tone due to compensatory dilatation, which might attenuate the extent of microvascular responsiveness to Ach. Hence, improved RBF and GFR responses to Ach might be partly secondary to restoration of basal vascular tone rather than endothelial function. Nevertheless, the greater improvement in MAP than RBF suggests that vascular resistance distal to the stenosis remained elevated.

We have previously shown that deterioration of renal hemodynamics and function in our RAS model is accompanied by oxidative stress, apoptosis, fibrosis, and inflammation.[6,7] In the current study, we observed that 4 weeks after PTRA, GFR and endothelial function improved, possibly secondary to the decrease in oxidative stress, as reflected in the downregulation of the expression of radical-producing enzyme, xanthine oxidase, thought to have an important role in renal ischemic injury.[18] Renal cell apoptosis was also reduced, suggesting reversal of renal 'hibernation'[16] in a kidney with preserved regenerative capacity.[19] Nevertheless, renal fibrosis induced by RAS was only partially improved after PTRA. As transforming growth factor-β and TIMP-1 were only slightly and not significantly upregulated by RAS, additional pro-fibrotic factors likely mediated renal

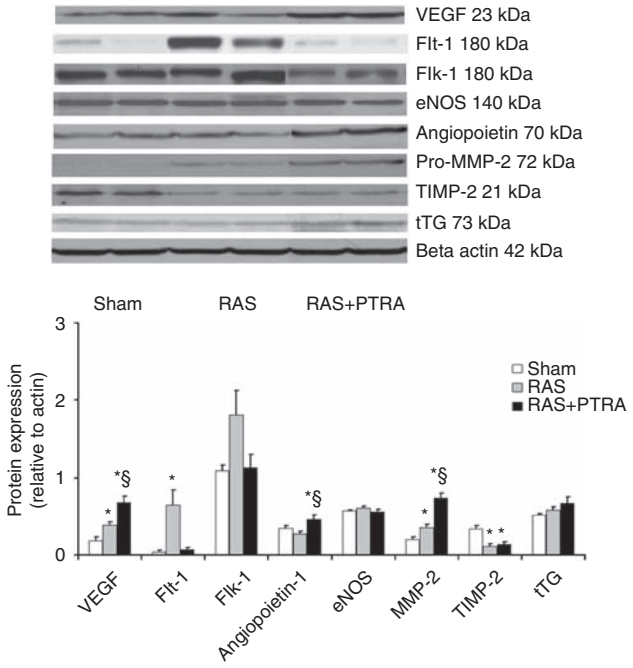

Figure 3 | Immunoblots (upper panel) and densitometric quantification (bottom) showing renal protein expression of vascular endothelial growth factor (VEGF), Flt-1, Flk-1, angiopoietin-1, endothelial nitric oxide synthase (eNOS), pro-matrix metalloproteinase (MMP)-2, tissue inhibitors of metalloproteinase 2 (TIMP-2) and tissue transglutaminase (tTG) in sham, renal artery stenosis (RAS), and RAS + percutaneous transluminal renal angioplasty (PTRA) groups. PTRA increased VEGF and angiopoietin-1 expression, suggesting a proangiogenic milieu in these kidneys. Mean ± s.e.m., $^{*}P<0.05$ vs sham, $^{\S}P<0.05$ vs RAS.

fibrosis in this model. Indeed, trichrome staining and the hydroxyproline assay showed an increase in renal collagen content induced by RAS. Moreover, connective tissue growth factor expression further increased after PTRA, trichrome staining was unaffected, and collagen content was not fully restored by PTRA, suggesting that the scarring process was incompletely arrested and that extracellular matrix deposited was not cleared from the kidney.

Furthermore, we have shown before that deterioration of renal function in RAS is associated with microvascular rarefaction and remodeling.[5–8] We suggested that angiogenic competence might be linked to renal functional recovery.[5] Neovascularization involves a sequence of events, such as endothelial cell proliferation, migration, differentiation, remodeling of extracellular matrix, and functional maturation of the newly assembled vessels, which are often mediated by VEGF.[20] Although the stenotic kidney showed elevated expression of VEGF, microvascular density was decreased. This might be partly due to the increased renal expression of the VEGF receptor Flt-1, which can sequester VEGF to decrease its activity and interfere with neovascularization.[21] Interestingly, we found that PTRA led to an increase in VEGF expression and microvascular density, especially in renal vessels $<40\,\mu m$ in diameter, which was accompanied by a slight increase of tortuousity, characteristic of angiogenic vessels, implying enhanced angiogenic efficacy.

The PTRA-induced neovascularization was likely mediated by interaction among several growth factors acting in concert. A decrease in Flt-1 might have contributed to an increase in effective VEGF availability, whereas the increase in renal expression of angiopoietin-1 in RAS + PTRA mediated maturation of the new vessels,[22] and the interaction between VEGF and angiopoietin-1 fostered microvascular stabilization. Matrix metalloproteinase-2 was increased in RAS + PTRA, and facilitated angiogenesis by degrading surrounding extracellular matrix and allowing endothelial cell invasion.[23] Taken together, our results indicate an important increase in proangiogenic milieu in the RAS kidney after PTRA, although with only partial restoration of the microvessels lost in RAS. These observations suggest that augmentations of the proangiogenic milieu in the post-stenotic kidney may offer the potential for new vessel formation in patients undergoing endovascular procedures.

It is important to recognize that microvascular vessel wall remodeling was not changed after PTRA and stenting, as indicated by the elevated media-to-lumen ratio. Moreover, the increased fraction of TUNEL-positive renal cells in RAS suggested increased apoptosis, as previously described,[7] which was underscored by activation of caspase-3, an important effector of apoptosis. PTRA diminished both TUNEL staining and activated caspase-3 expression, implying attenuation of the apoptotic process by PTRA. Nevertheless, caspase-3 expression did not return to sham levels after PTRA, both renal interstitial fibrosis and microvascular remodeling were not restored, and neovascularization was incomplete. This study therefore shows curtailed structural recovery 4 weeks after PTRA, which may, in part, account for the mere partial restoration of RBF in the stenotic kidney. In most patients with nonatherosclerotic RAS, technically successful PTRA is followed by a prompt decrease in blood pressure within 1–6 h; in 93% it has stabilized within 24 h, and remains stable at 6 months.[24] Indeed, we observed that blood pressure in RAS started decreasing shortly after PTRA. We would expect to observe improvement in renal function by 4 weeks after PTRA, because an increase in GFR in human RAS has been documented within 5 days after angioplasty,[13] but may occur even earlier in parallel to MAP. Furthermore, a recent study in patients with RAS showed significant improvement in endothelial function and a decrease in blood pressure and oxidative stress by 1 month after angioplasty.[12] Therefore, our observation that 4 weeks after PTRA GFR increased while RBF and the renal microcirculation remained impaired, likely bears clinical relevance.

Our study was limited by the use of pigs without comorbid conditions, and by a short duration of RAS relative to the human disease. Human RAS is multifactorial and particularly dependent on the severity, evolution, and duration of the stenosis, as well as on other concurrent or preexisting pathophysiological conditions such as essential hypertension, diabetes, or hypercholesterolemia,

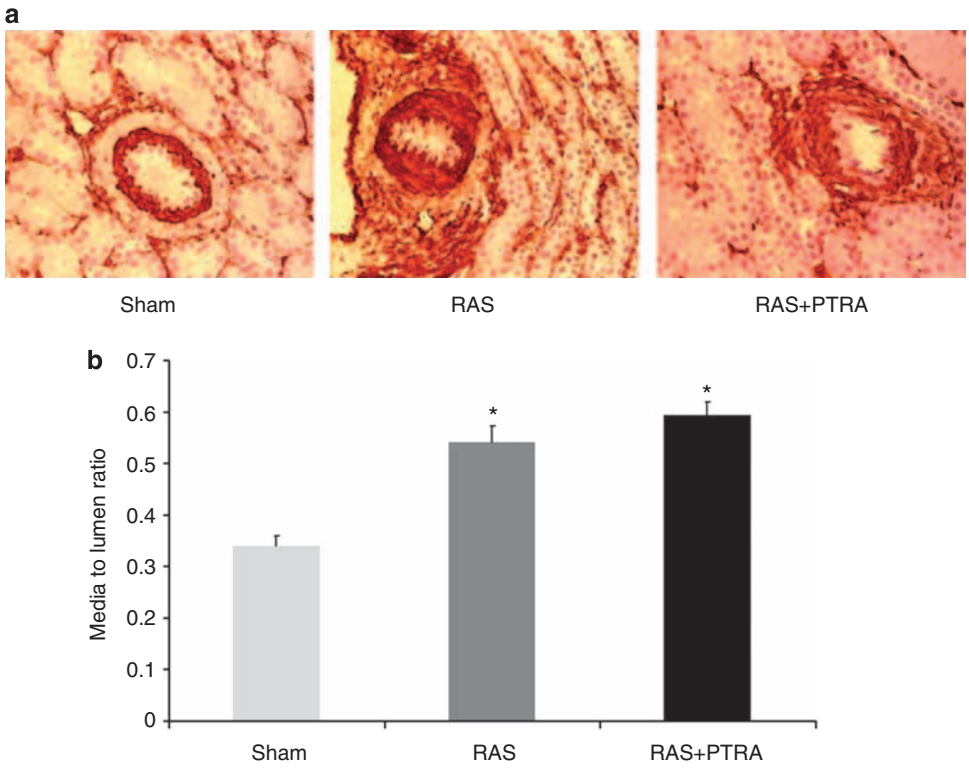

Figure 4 | Microvascular remodeling in the stenotic kidney. (**a**) Representative renal α-smooth muscle actin staining in sham, renal artery stenosis (RAS), and RAS + percutaneous transluminal renal angioplasty (PTRA) kidneys. (**b**) Quantification of media-to-lumen ratio (mean ± s.e.m.) in the same groups. *$P < 0.001$ vs sham.

which impair the renal microvasculature and likely modulate its response to revascularization. Nevertheless, renal structure and function in the swine model are similar to human kidneys, and our results bear relevance and may shed light on the reversibility of renal injury after revascularization.

In conclusion, the present study shows that PTRA in chronic porcine RAS partially restored the renal microvascular network and allowed GFR recovery. However, our study suggests that the improvement in GFR and decrease in blood pressure 4 weeks after PTRA may conceal residual structural damage even in the post-stenotic kidney uncomplicated by atherosclerosis. These observations suggest that the improvement in renal function can precede or be achieved without complete eradication of renal scarring. Future studies will need to determine whether such residual damage might resolve, interfere with renal functional reserve, or predispose the kidney for future injury.

MATERIALS AND METHODS

Experimental protocol and multidetector computer tomography analysis

The institutional Animal Care and Use Committee approved all the procedures. In all, 21 female domestic pigs (45–68 kg) were studied after 10 weeks of observation. At baseline, all the pigs were anesthetized with an intramuscular injection of telazol (5 mg/kg) and xylazine (2 mg/kg), intubated, and mechanically ventilated with room air. Anesthesia was maintained with a mixture of ketamine (0.2 mg/kg/min) and xylazine (0.03 mg/kg/min) in normal saline (0.05 µl/kg/min). In 13 pigs, RAS was induced at baseline by a local-irritant coil placed in the main renal artery, inducing gradual development of unilateral RAS by 5–7 days, as described previously.[9,25,26] A PhysioTel telemetry system (Data Sciences International, Arden Hills, MN, USA) was implanted on the same day in a femoral artery to continuously monitor MAP in all animals.[25,26] MAP was recorded at 5-min intervals and averaged for each 24-h period. Levels reported in Table 1 were those obtained for 2 days preceding the *in vivo* studies.

At 6 weeks after induction of RAS, the pigs were anesthetized again and randomized into two groups that underwent either sham treatment (RAS, $n = 7$) or PTRA (RAS + PTRA, $n = 6$). The degree of stenosis was evaluated by selective renal angiography, followed by PTRA or sham procedure. A 7F balloon catheter was engaged in the proximal-middle section of the renal artery under fluoroscopic guidance and the balloon was inflated, resulting in expansion of a tantalum stent to full balloon diameter, to restore luminal opening. Then, the balloon was deflated and removed, leaving the stent embedded in the vascular wall. A group of normal kidneys that did not undergo coil implantation served as controls (sham, $n = 8$).

The pigs were again anesthetized similarly, 4 weeks later. Blood samples were collected from the inferior vena cava for the measurement of plasma renin activity (radio-immunoassay) and creatinine (colorimetric assay).[8] Single-kidney renal function was then evaluated *in vivo* using helical multidetector computer tomography for assessment of basal regional renal perfusion, RBF, and GFR, as previously described in detail.[5–7,27,28] Briefly, this method was performed with sequential acquisition of 160

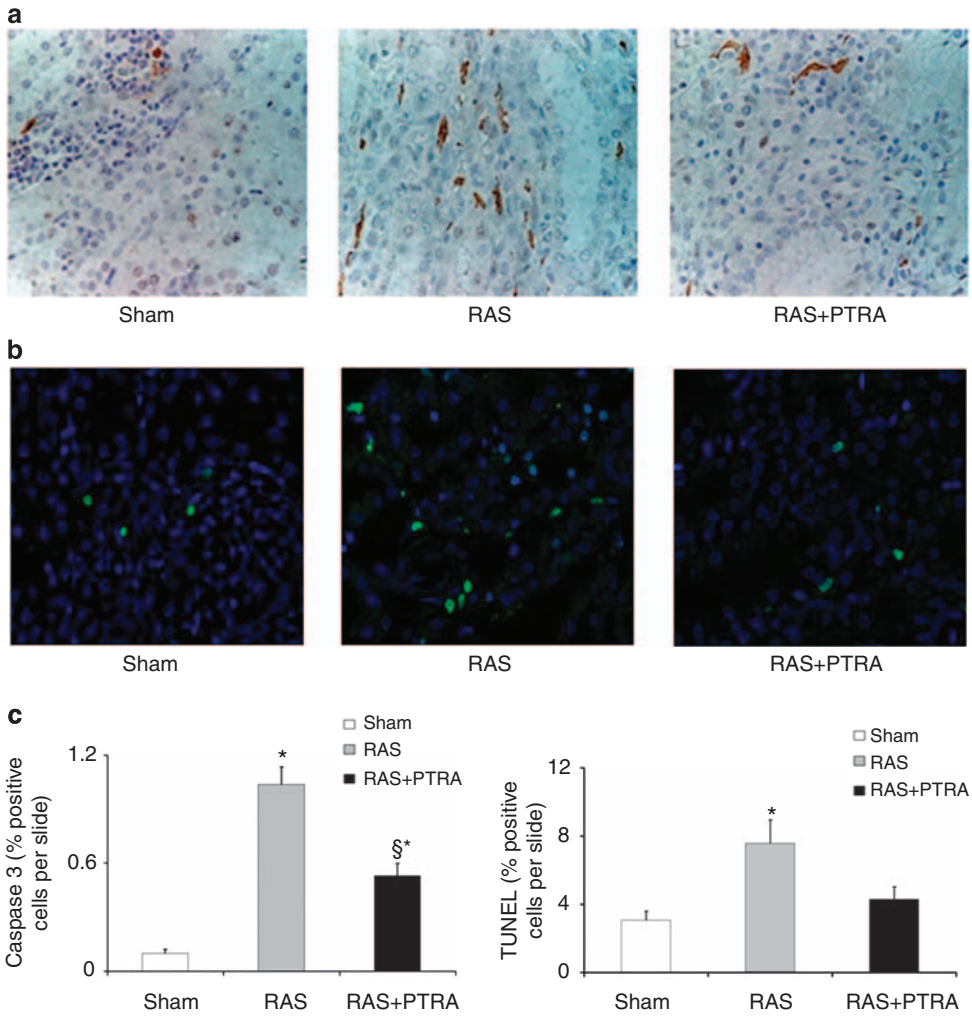

Figure 5 | Apoptosis in the stenotic kidney, and response to revascularization. Caspase-3 (**a**, brown) and terminal deoxynucleotidyl transferase dUTP nick end labeling (TUNEL) (**b**, green) staining and quantification (**c**), showing increased number of positive (apoptotic signal) cells in renal artery stenosis (RAS), which was decreased after percutaneous transluminal renal angioplasty (PTRA). *$P < 0.01$ vs sham; §$P < 0.01$ vs RAS.

consecutive scans over a period of almost 3 min after a central venous injection of iopamidol (0.5 ml/kg for 2 s). Multidetector computer tomography images were reconstructed and displayed with the Analyze software package (Biomedical Imaging Resource, Mayo Clinic, MN, USA). Regions of interest were selected from cross-sectional images from the aorta, renal cortex, and medulla. Average tissue attenuation in each region was plotted over time and fitted by curve-fitting algorithms to obtain measures of renal function. Cortical and medullary volumes were calculated by Analyze (Biomedical Imaging Resource, Mayo Clinic, MN, USA) and RBF as the sum of the products of cortical and medullary perfusions and corresponding volumes. GFR was calculated from the cortical curve using the slope of the proximal tubular curve. The same procedure was repeated after 15 min toward the end of a 10-min suprarenal infusion of Ach (5 μg/kg/min) to test endothelium-dependent microvascular reactivity. Briefly, a tracker catheter (Prowler Microcatheter, Cordis, Miami, FL, USA) introduced from the carotid artery was placed above the renal arteries for infusion of Ach. Hemodynamics and function were therefore measured over a stable 3-min observation period at baseline and during Ach infusion.

Few days after completion of all functional studies, the pigs were killed (100 mg/kg sodium pentobarbital). Kidneys were removed, immersed in 4°C saline solution containing heparin (10 U/ml), and divided into different lobes, and stored at −80°C by immersing them in 10% buffered formalin, or cannulated and prepared for micro-computed tomography analysis.

Micro-computed tomography analysis

All kidneys were perfused with 0.9% saline (containing heparin) at 10 ml/min under physiological perfusion pressure (100 mm Hg), using a saline-filled cannula ligated in a segmental artery. After 5–10 min, this was replaced with an intravascular radio-opaque silicone polymer (Microfil MV122; Flow Tech, Carver, MA, USA; 0.8 ml/min) until the polymer drained freely from the segmental vein. A lobe of the polymer-filled tissue was subsequently trimmed, prepared and encased in paraffin, and scanned at 0.5° increments using a micro-computed tomography scanner, as described previously.[8] Three-dimensional volume images were then reconstructed at cubic voxels of 20 μm on a side, and displayed at 40-μm cubic voxels for analysis. The spatial density, average diameter, and

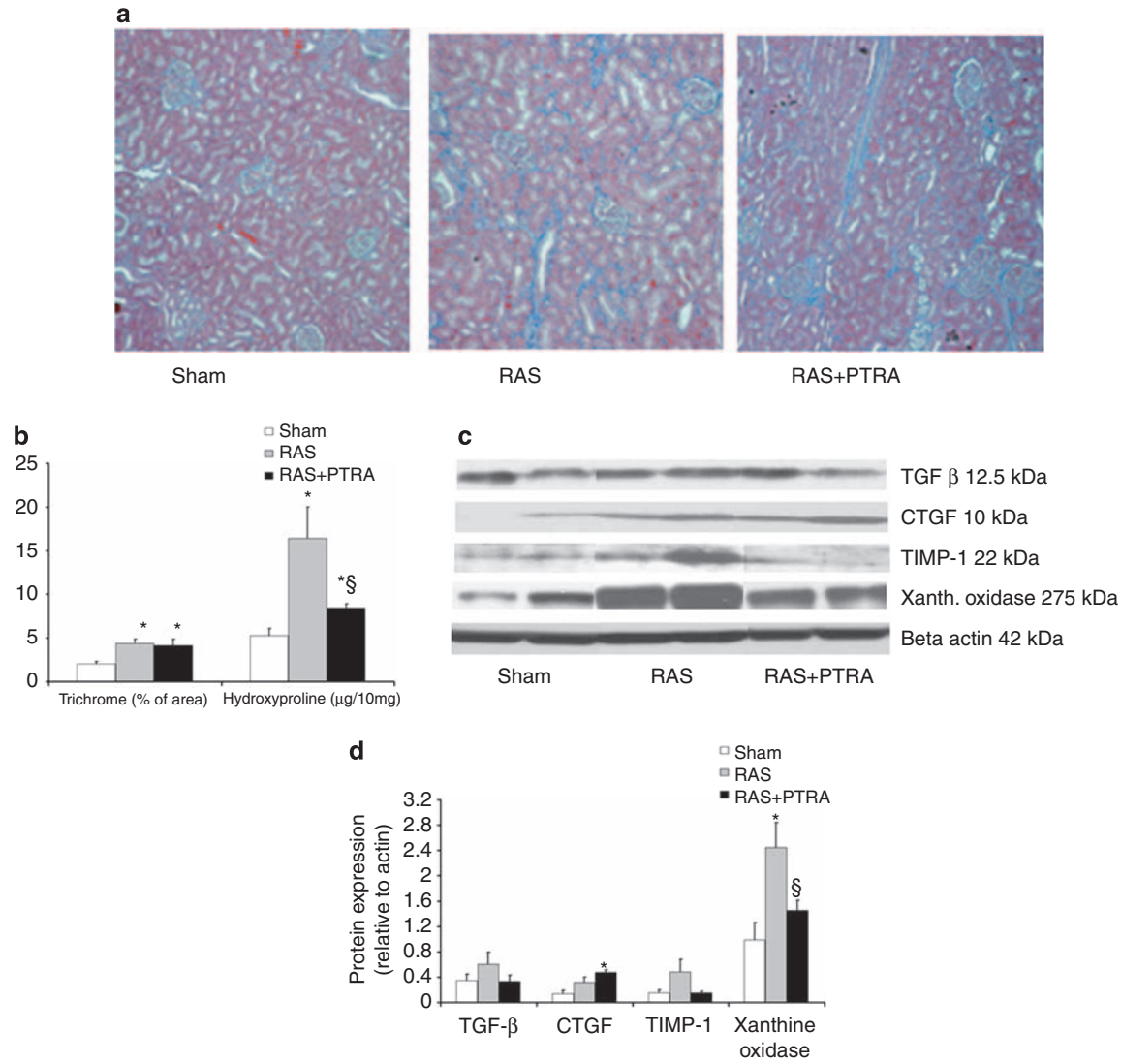

Figure 6 | Stenotic kidney fibrosis and oxidative stress. Representative images of trichrome (**a**) and quantification (**b**) of trichrome and hydroxyproline (mean ± s.e.m.) in sham, renal artery stenosis (RAS), and RAS + percutaneous transluminal renal angioplasty (PTRA) groups. Immunoblots (**c**) and densitometric quantification (**d**) showing renal protein expression of transforming growth factor (TGF)-β, connective tissue growth factor (CTGF), tissue inhibitors of metalloproteinase 1 (TIMP-1), and xanthine oxidase in sham, RAS, and RAS + PTRA groups; mean ± s.e.m., $^{*}P<0.05$ vs sham, $^{\S}P<0.05$ vs RAS.

tortuousity of cortical microvessels were calculated as we have previously described,[8,29] and classified according to diameter as small (<40 μm), medium (40–100 μm), or large (>100 μm) vessels.

Immunohistochemistry and western blotting

In vitro studies were performed to assess mechanisms responsible for formation and maintenance of the renal microvasculature, as well as fibrogenic factors and oxidative stress in the kidney. Standard western blotting protocols were performed[7] with specific antibodies previously used or that cross-react with swine tissue. We used antibodies against VEGF, its receptors Flt-1 and Flk-1, angiopoietin-1, endothelial nitric oxide synthase, matrix metalloproteinase-2, transforming growth factor-β, TIMP-1 and TIMP-2 (1:200, Santa Cruz Biotechnology, Santa Cruz, CA, USA), and tissue transglutaminase (1:1000, Abcam, Cambridge, MA, USA). To assess representative mediators of oxidative stress, protein expression of xanthine oxidase (1:10,000, Chemicon International, Temecula, CA, USA) was also evaluated. β-actin (1:3000, Sigma, St Louis, MO, USA) was used as loading control.

Staining was performed in 5 μm paraffin slides for Masson trichrome and α-smooth muscle actin (1:50, Sigma), or in frozen slides for activated caspase-3 (1:200, Santa Cruz), following standard procedures.[5,27] Each representative staining was quantified semi-automatically in 13 fields, expressed as percentage of staining of total surface area or number of positive cells per slide. The microvascular media-to-lumen ratio was measured in α-smooth muscle actin-positive microvessels under 500 μm in diameter. Apoptotic signals were characterized in renal cells with the TUNEL method using the DeadEnd Fluorometric TUNEL system (Promega, Madison, WI, USA), as we have previously shown.[8] Apoptotic cells were quantified in 15 fields as the fraction of TUNEL-positive nuclei in each field.

Collagen content

The kidney cortex of each animal was used for hydroxyproline assay as described previously.[30] Briefly, the cortex was weighed, minced, homogenized, and diluted in phosphate-buffered saline to 100 mg cortex weight per ml. Samples (100 µl) were then hydrolyzed in 12 mol/l HCl and duplicate samples analyzed by hydroxyproline assay.

Statistical analysis

Quantitative data are expressed as mean ± s.e.m. We tested Gaussian distribution using Kolmogorov–Smirnov test and equality of variances with Bartlett test. Statistical comparisons among different experimental groups or studies were subsequently performed using one-way analysis of variance with Newman–Keuls *post hoc* test or nonparametric Kruskal–Wallis one-way analysis of variance by ranks test with Dunns *post hoc* test. Paired *t*-test was used for comparison within groups. Statistical significance was accepted for $P \leqslant 0.05$.

DISCLOSURE

All the authors declared no competing interests.

ACKNOWLEDGMENTS

This study was partly supported by grant numbers DK-73608, DK-77013, HL-77131, and PO1HL-085307 from the NIH. FF was supported by a grant from Fondation Transplantation (France).

REFERENCES

1. Garovic VD, Textor SC. Renovascular hypertension and ischemic nephropathy. *Circulation* 2005; **112**: 1362–1374.
2. Textor SC, Lerman L, McKusick M. The uncertain value of renal artery interventions: where are we now? *JACC Cardiovasc Interv* 2009; **2**: 175–182.
3. Dubel GJ, Murphy TP. The role of percutaneous revascularization for renal artery stenosis. *Vasc Med* 2008; **13**: 141–156.
4. Textor SC. Ischemic nephropathy: where are we now? *J Am Soc Nephrol* 2004; **15**: 1974–1982.
5. Chade AR, Zhu X, Mushin OP *et al.* Simvastatin promotes angiogenesis and prevents microvascular remodeling in chronic renal ischemia. *FASEB J* 2006; **20**: 1706–1708.
6. Chade AR, Rodriguez-Porcel M, Grande JP *et al.* Distinct renal injury in early atherosclerosis and renovascular disease. *Circulation* 2002; **106**: 1165–1171.
7. Chade AR, Rodriguez-Porcel M, Grande JP *et al.* Mechanisms of renal structural alterations in combined hypercholesterolemia and renal artery stenosis. *Arterioscler Thromb Vasc Biol* 2003; **23**: 1295–1301.
8. Zhu XY, Chade AR, Rodriguez-Porcel M *et al.* Cortical microvascular remodeling in the stenotic kidney: role of increased oxidative stress. *Arterioscler Thromb Vasc Biol* 2004; **24**: 1854–1859.
9. Lerman LO, Schwartz RS, Grande JP *et al.* Noninvasive evaluation of a novel swine model of renal artery stenosis. *J Am Soc Nephrol* 1999; **10**: 1455–1465.
10. Chade AR, Zhu X, Lavi R *et al.* Endothelial progenitor cells restore renal function in chronic experimental renovascular disease. *Circulation* 2009; **119**: 547–557.
11. Lerman LO, Nath KA, Rodriguez-Porcel M *et al.* Increased oxidative stress in experimental renovascular hypertension. *Hypertension* 2001; **37**: 541–546.
12. Higashi Y, Sasaki S, Nakagawa K *et al.* Endothelial function and oxidative stress in renovascular hypertension. *N Engl J Med* 2002; **346**: 1954–1962.
13. Airoldi F, Palatresi S, Marana I *et al.* Angioplasty of atherosclerotic and fibromuscular renal artery stenosis: time course and predicting factors of the effects on renal function. *Am J Hypertens* 2000; **13**: 1210–1217.
14. Hansen KJ, Edwards MS, Craven TE *et al.* Prevalence of renovascular disease in the elderly: a population-based study. *J Vasc Surg* 2002; **36**: 443–451.
15. Xia J, Seckin E, Xiang Y *et al.* Positron-emission tomography imaging of the angiotensin II subtype 1 receptor in swine renal artery stenosis. *Hypertension* 2008; **51**: 466–473.
16. Lerman L, Textor SC. Pathophysiology of ischemic nephropathy. *Urol Clin North Am* 2001; **28**: 793–803, ix.
17. Pipinos II, Nypaver TJ, Moshin SK *et al.* Response to angiotensin inhibition in rats with sustained renovascular hypertension correlates with response to removing renal artery stenosis. *J Vasc Surg* 1998; **28**: 167–177.
18. Greene EL, Paller MS. Xanthine oxidase produces O2-. in posthypoxic injury of renal epithelial cells. *Am J Physiol* 1992; **263**: F251–F255.
19. Cheung CM, Shurrab AE, Buckley DL *et al.* MR-derived renal morphology and renal function in patients with atherosclerotic renovascular disease. *Kidney Int* 2006; **69**: 715–722.
20. Griffioen AW, Molema G. Angiogenesis: potentials for pharmacologic intervention in the treatment of cancer, cardiovascular diseases, and chronic inflammation. *Pharmacol Rev* 2000; **52**: 237–268.
21. Fischer C, Mazzone M, Jonckx B *et al.* FLT1 and its ligands VEGFB and PlGF: drug targets for anti-angiogenic therapy? *Nat Rev Cancer* 2008; **8**: 942–956.
22. Baffert F, Le T, Thurston G *et al.* Angiopoietin-1 decreases plasma leakage by reducing number and size of endothelial gaps in venules. *Am J Physiol Heart Circ Physiol* 2006; **290**: H107–H118.
23. Jackson C. Matrix metalloproteinases and angiogenesis. *Curr Opin Nephrol Hypertens* 2002; **11**: 295–299.
24. Birrer M, Do DD, Mahler F *et al.* Treatment of renal artery fibromuscular dysplasia with balloon angioplasty: a prospective follow-up study. *Eur J Vasc Endovasc Surg* 2002; **23**: 146–152.
25. Chade AR, Rodriguez-Porcel M, Herrmann J *et al.* Antioxidant intervention blunts renal injury in experimental renovascular disease. *J Am Soc Nephrol* 2004; **15**: 958–966.
26. Chade AR, Krier JD, Rodriguez-Porcel M *et al.* Comparison of acute and chronic antioxidant interventions in experimental renovascular disease. *Am J Physiol Renal Physiol* 2004; **286**: F1079–F1086.
27. Chade AR, Bentley MD, Zhu X *et al.* Antioxidant intervention prevents renal neovascularization in hypercholesterolemic pigs. *J Am Soc Nephrol* 2004; **15**: 1816–1825.
28. Daghini E, Primak AN, Chade AR *et al.* Assessment of renal hemodynamics and function in pigs with 64-section multidetector CT: comparison with electron-beam CT. *Radiology* 2007; **243**: 405–412.
29. Zhu XY, Rodriguez-Porcel M, Bentley MD *et al.* Antioxidant intervention attenuates myocardial neovascularization in hypercholesterolemia. *Circulation* 2004; **109**: 2109–2115.
30. Dixon IM, Hao J, Reid NL *et al.* Effect of chronic AT(1) receptor blockade on cardiac Smad overexpression in hereditary cardiomyopathic hamsters. *Cardiovasc Res* 2000; **46**: 286–297.